



## Article

# Fractal Operators and Fractional Dynamics with 1/2 Order in Biological Systems

Yajun Yin <sup>1,\*</sup> , Jianqiao Guo <sup>2</sup>, Gang Peng <sup>1</sup> , Xiaobin Yu <sup>1</sup> and Yiya Kong <sup>3,4</sup>

- <sup>1</sup> Department of Engineering Mechanics, Tsinghua University, Beijing 100084, China; pg16@mails.tsinghua.edu.cn (G.P.); yxb18@mails.tsinghua.edu.cn (X.Y.)
- <sup>2</sup> MOE Key Laboratory of Dynamics and Control of Flight Vehicle, School of Aerospace Engineering, Beijing Institute of Technology, Beijing 100081, China; guojianqiao@bit.edu.cn
- <sup>3</sup> Department of Cardiology, Beijing Hospital, National Center of Gerontology, Institute of Geriatric Medicine, Chinese Academy of Medical Sciences, Beijing 100730, China; yiykong@163.com
- <sup>4</sup> Graduate School, Peking Union Medical College, Beijing 100005, China
- \* Correspondence: yinyj@mail.tsinghua.edu.cn

**Abstract:** This paper reports the new advances in biological fractal dynamics. The following contents are included: (1) physical (or functional) fractal spaces abstracted from biological materials, biological structures and biological motions; (2) fractal operators on fractal spaces; (3) 1/2-order fractional dynamics controlled by fractal operators; and (4) the origin of 1/2-order. Based on the new progress, we can make a judgment that all the two-bifurcation physical functional fractal motions in the living body can be attributed to the fractional dynamics with 1/2-order.

**Keywords:** physical (functional) fractal space; fractal operators; fractional order dynamics; 1/2-order



**Citation:** Yin, Y.; Guo, J.; Peng, G.; Yu, X.; Kong, Y. Fractal Operators and Fractional Dynamics with 1/2 Order in Biological Systems. *Fractal Fract.* **2022**, *6*, 378. <https://doi.org/10.3390/fractalfract6070378>

Academic Editor: Corina S Drapaca

Received: 25 May 2022

Accepted: 26 June 2022

Published: 2 July 2022

**Publisher's Note:** MDPI stays neutral with regard to jurisdictional claims in published maps and institutional affiliations.



**Copyright:** © 2022 by the authors. Licensee MDPI, Basel, Switzerland. This article is an open access article distributed under the terms and conditions of the Creative Commons Attribution (CC BY) license (<https://creativecommons.org/licenses/by/4.0/>).

## 1. Introduction

This paper focuses on fractal operators and fractional dynamics in biomaterials, biological structures and motions. In recent years, we have studied the following problems in biomechanics and biophysics: the first one is the constitutive response of muscle and ligament fibers [1]; the second one is the electrical signal transduction within nerve fibers [2], and the third one is the blood flow in arterial vessels [3]. Ultimately, it was astonishing to find that the three types of problems show surprising commonality, i.e., their basic laws can all be inscribed by fractal operators, and their mechanics are all 1/2-order fractional dynamics.

The objects studied are completely different. The research fields are completely different. The scientific laws obeyed are also completely different. However, amazing consistency is displayed. How can this consistency be understood? Is the consistency a coincidence or a logical necessity? Furthermore, is this consistency of universality within living organisms? Does it exist in other life motions? This paper is dedicated to finding the answers.

It is noted that the above three kinds of biophysical mechanical phenomena can be attributed to the two-bifurcation physical function fractal movement. It is the source of the 1/2-order fractional time differential dynamic response of biological systems, and that is what we are looking for. Together, they show universal laws of biological systems.

Fractals and fractional orders are different concepts. The difference between fractal and fractional order in a biological system simulation is that fractals in a traditional biomechanical simulation is all about fractals in geometric structure, for example, fractals of vascular tree shape structure [4]. The fractional order, which is embodied in the differential governing equations that regulate biomechanical phenomena, is the fractional differential of non-integer calculus [5,6]. However, the physical functional fractals proposed in this paper are different from the classical fractals. They have fractal characteristics but not geometric ones. They are functional physical fractals, whose physical laws meet the

distribution characteristics of fractal structures, and they reflect the correlation between physical fractals and fractional time-differential dynamic responses.

Moreover, the functional physical fractal structure proposed by us contains specific physical meanings and represents the physical time differential response characteristics; we mainly discuss the time fractional operator.

## 2. Fractalization Ideology and Physical Fractal Space

We carefully compare the basic ideas in the literature [1–3]. We find that the three papers are exactly based on the same idea of fractalization. With the fractalization ideology as the basis, we can develop a completely consistent form of physical fractal space.

The three types of problems addressed in the literature [1–3] are not novel. In the past, all these problems have been studied systematically [7–14]. Kasteltic et al. studied the multistage structure and physical mechanical properties of biological fibers [7–12]. Chaudhuri and Joglekar explored the multistage circuit model of biological cortical nerve fibers to simulate neural signal transmission [13,14]. Burattini, Abdolrazaghi and Goldwyn studied the electrical analogy structure model of a biological artery to simulate hemodynamic behavior [15–17]. They all use a particular structural model to study a particular biophysical phenomenon. However, none of the past studies has broken through the classical spatial form. The specific explanations are as follows.

The classical biofiber mechanics are studied in Euclid space. The Euclid geometry is drawn on to inscribe the properties and mechanical response of fibers. In appearance, the spatial form is not involved in nerve fiber electrical signal transduction, but when analyzed in depth, it can be seen that the Euclid geometry appears in a covert way in signal transduction theory. As for hemodynamics, it is considered as a branch of fluid mechanics in mechanics. Blood flows in Euclid space, and its geometric basis is undoubtedly Euclidean [15–17].

Unlike the classical studies, the studies [1–3] introduce a unique fractal space. For ease of understanding, the biological fiber (Figure 1) in the literature [1] is used as the study subject to show the abstraction process of fractal space.

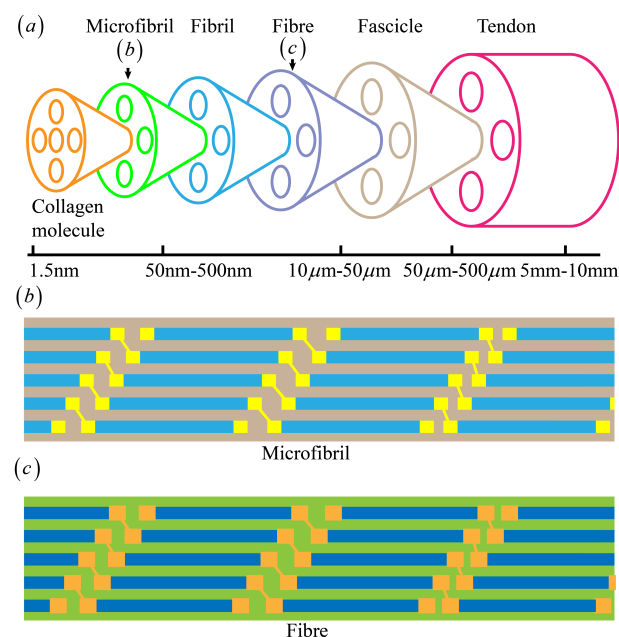


**Figure 1.** Self-similar structure in tendon. (a) Multilevel structure of tendon; (b) Arrangement of microfibril; (c) Arrangement of macro-fiber.

Figure 1a shows the self-similar multilevel structure of the tendon. Figure 1b displays a microfibril formed by the arrangement of molecular collagen chains, and Figure 1c shows

a macro-fibril formed by the arrangement of protofibril chains. The microfibril shows considerable similarity to the macro-fibril. Refs. [18,19] show that the multilevel self-similarity is exactly the basic feature of the fractal structure. It should be noted that this multilevel structural self-similarity is a geometrical one. Such a fractal with geometric self-similarity is termed a geometric fractal. It can be concluded that most of the fractals we have seen in textbooks so far are geometric fractals.

However, the fractals in the literature [1–3] are not purely geometric. The structure in Figure 1b is abstracted as follows. A microfibril consists of many molecular chains stacked together. One of the molecular chains is isolated and reduced to a straight chain (Figure 2). The straight chain is embedded in the gel substrate. Once the straight chain is stressed, it will be deformed elastically. The collagen molecule can be regarded as an elastic element with the elastic module  $k$ . The interaction between collagen molecules and the gel substrate leads to a shear-lag effect, which can be portrayed by viscous components with the viscosity denoted as  $\mu$ . Thus, the transfer of forces and deformations along the straight chain and the substrate can be described by the combination of the two elements.

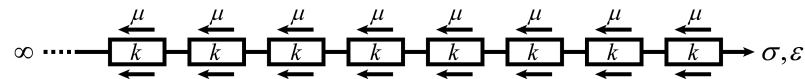


**Figure 2.** Straight chain of molecules abstracted from microfibrils.

Based on the transfer path of forces and deformations along the straight chain, it can be found that the elements obey the following rules:

1. The elastic element  $k$  is connected in parallel with the viscous element  $\mu$  to produce the first-level structure;
2. Copy the first-level structure to generate the second-level structure;
3. The second-level structure is connected in series with the elastic element  $k$  in the first level;
4. Copy the second-level structure to generate the third-level structure;
5. The third-level is connected in series with the elastic element  $k$  of the second level;
6. Repeat the above steps.

In this way, repeating the above generation rules generates a bifurcated multilevel tree structure (Figure 3), which is termed as the component tree. Since the  $(i + 1)$ th-level structure perfectly replicates the  $i$ th-level structure, the adjacent two levels of the component tree are congruence, and the multilevel structure has a perfect self-identical character in the whole.

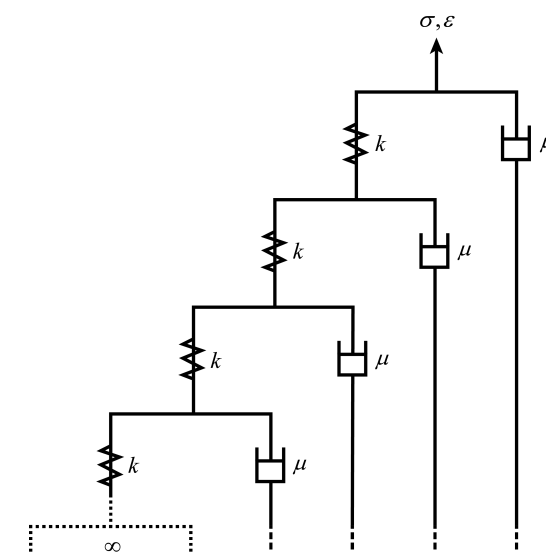


**Figure 3.** The fractal tree of self-identical components abstracted from the straight chain.

If the number of levels of the multilevel structure tends to infinity, the self-identical component tree becomes a special fractal tree (see Figure 3). Interestingly, the fractal structure in Figure 3 differs from those in the textbook. Conventional regular fractals in the textbook are characterized by infinite-level self-similarity, while the fractal tree in Figure 3 is characterized by infinite-level self-identity. Self-identity is a special form of self-similarity. The fractal structure with self-identity is so far one of the most special forms of fractals.

The fractals in the textbook are constructed by geometric elements, so they can be termed geometric fractals, and the corresponding space is geometric fractal space. The fractal tree in Figure 3 is constructed by physical elements, so it is termed a “physical fractal”, and the corresponding space is physical fractal space or element fractal space. Since the element fractal space carries specific mechanical or biological functions, it can also be named functional fractal space.

There is an essential difference between physical fractals and geometric fractals [1,2,20,21]. Geometric fractal space requires the definition of metrics, and the natural laws there are controlled by scaling laws. However, physical fractal space does not necessarily need metrics. The natural laws on physical fractal spaces can be inscribed without scaling laws.

Obviously, there cannot be an infinite number of collagen molecules in the chain shown in Figure 3, and therefore, an infinite-level structure in physics or biology does not exist. However, this does not prevent us from generalizing the finite level to an infinite level that is just an idealized limited state. In scientific exploration, the objects studied are often pushed to extreme states for the sake of simplicity. The studies [1–3] have demonstrated that the behaviors of infinite-level structures are much simpler and more effective than those of finite-level structures. This suggests that infinite-level structure, although an idealized product, does capture the essence of the matters.

The above fractalization ideology, although refined from Ref. [1], shows its power in the literature [2,3]. Ref. [1] fractalized the force and deformation transmission in tendon fibers, Ref. [2] fractalized the electrical signal transmission in nerve fibers, and Ref. [3] fractalized the arterial blood flow in vessels. Based on fractalization, it can be said that physical fractal space exists not only in tendon fibers but also in nerve fibers and arterial blood flows. We are optimistic to say that the ideology of fractalization should be of universality in living organisms and that physical fractal space should be a universal space form. We will examine the universality of the fractalization idea in the subsequent chapters. Up to now, we are able to glimpse the origins of the consistency in the studies [1–3].

### 3. Fractal Operators and Their Algebraic Equations on Physical Fractal Spaces

Once the physical fractal space is abstracted, kinetics analysis in the space could be performed. However, since fractal spaces have an infinite number of levels, it would be tedious to perform operations level by level. This leads to the question: how do we achieve concise and fast operations on physical fractal spaces? To this end, we have developed the concepts of fractal cells and fractal operators in the studies [1–3]. The concept of a fractal cell first appeared in [1]. Now, the idea of a fractal cell is refined further as follows.

The fractal tree generated by the elastic component  $k$  and viscous component  $\mu$  can be overall physically equivalent to a single fractal element  $F$  (Figure 4a). That is, the overall component fractal tree can be set into a fractal element  $F$ .

If the fractal tree is checked from a different way, in which one stands on the first elastic element  $k$  and looks toward the second level of the structure, then another fractal tree (or another fractal element  $F$ ) will be found. Thus, the entire fractal tree is equivalent to such a structure that the first elastic element  $k$  is connected in series with the fractal element  $F$  and then in parallel with another viscous element  $\mu$ . The equivalent structure involved with  $k$ ,  $\mu$ , and  $F$ , is the fractal cell (Figure 4a).

Thus, logically, the fractal tree is equivalent to both the fractal element  $F$  and the fractal cell, and it immediately follows that the fractal cell must be equivalent to the fractal element  $F$ , which is the meaning of the equal sign “=” in Figure 4a. This sign “=” implies that there is an invariance on the physical fractal space, i.e., the equivalence of fractal cell and fractal

element  $F$ . This equivalence, which is an intrinsically invariant property of the physical fractal space, is thus of essential importance.

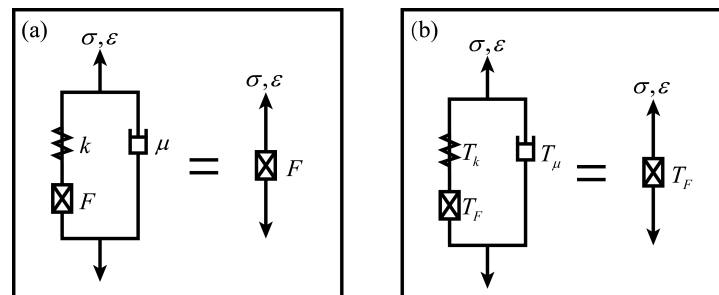


**Figure 4.** Equivalence of structural elements and fractal operators of cell elements of functional fractal trees. (a) Equivalence of component fractal tree with fractal cell and fractal element; (b) The invariance of the operator fractal space.

Dynamical responses of physical components can be characterized by operators. Operators defined on physical elements are termed element operators, e.g., elastic element operator  $T_k$  and viscous element operator  $T_\mu$ . Operators defined on the fractal element  $F$  (i.e., component fractal trees) are termed fractal element operator  $T_F$ , or they are abbreviated as fractal operator. If the stress on a general element is  $\sigma$ , with the strain  $\varepsilon$  and the module  $G$ , respectively, then we have:

$$\sigma = T\varepsilon, \quad (1)$$

For the elastic element  $k$ , we have:

$$T = T_k = G. \quad (2)$$

For the viscous element  $\mu$ , we have

$$T = T_\mu = G\lambda p, \quad (3)$$

where  $\lambda$  is the relaxation time constant, and  $p$  is denoted as the classic time differential operator given by

$$p = \frac{d}{dt}. \quad (4)$$

For the fractal element  $F$ , we have

$$T = T_F, \quad (5)$$

here, the fractal operator  $T_F$  is the unknown operator to be solved.

Based on the equilibrium equation, deformation compatibility equation in mechanics and the operator algebra [22,23], it can be confirmed that the invariance inscribed by the sign = in Figure 4b still holds when the components are replaced by the corresponding operators (Figure 4b). If Figure 4a shows the invariance of the component fractal space, it can be said that Figure 4b shows the invariance of the operator fractal space. The invariance of the operator fractal space provides the algebraic equation satisfied by the operators

$$\frac{1}{\frac{1}{T_F} + \frac{1}{T_k}} + T_\mu = T_F. \quad (6)$$

In mechanics, the right-hand side (RHS) of Equation (6) can be considered as the stiffness of the fractal element  $F$ , and the left-hand side (LHS) can be considered as the

stiffness of the fractal cell element. The fractal cell element has two branches, so its stiffness is the sum of the stiffnesses of the two branches. Furthermore, Equation (6) may lead to

$$T_F^2 - T_\mu T_F - T_\mu T_k = 0. \quad (7)$$

Equation (7) is the algebraic equation for the fractal operator  $T_F$ . There exists a radical solution below

$$T_F = \frac{T_\mu \pm \sqrt{T_\mu^2 + 4T_\mu T_k}}{2}. \quad (8)$$

At this step, the fractal operator  $T_F$  is determined.

#### 4. Why Is the 1/2 Order?

The answer is simple: because the fractal operator  $T_F$  satisfies the 2nd algebraic equation Equation (7) and its solution contains the 2nd root term  $\sqrt{T_\mu^2 + 4T_\mu T_k}$  in Equation (8). So, it is said that the fractal operator  $T_F$  is an operator with order 1/2 apparently. Here, the qualifier apparently is added because the final order of the root term  $\sqrt{(\cdot)}$  depends not only on the apparent sign  $\sqrt{\cdot}$  but also on the order of the operator  $(\cdot)$ .

Once the fractional operator  $T_F$  (i.e., fractal operator) acts on the function  $\varepsilon$ , i.e.,  $T_F \varepsilon$ , immediately, fractional calculus will occur. Therefore, we say that the dynamics controlled by the fractional operator  $T_F$  is apparently the fractional dynamics with order 1/2. Here, we propose the functional physical fractal structure, which itself contains specific physical meaning, and it represents the physical time differential response characteristics. Therefore, we apply the time fractional operator.

This answer is still not satisfactory. So, we continue to inquire why it is the quadratic algebraic equation. It is noted that the physical fractal space in Figure 3 can be regarded as a topological space, while the fractal tree and its corresponding fractal cell has a two-bifurcation topology. As mentioned above, each bifurcation corresponds to a stiffness term, and two bifurcations correspond to two stiffness terms, as shown in Equation (6). It is noted that every stiffness term is indispensable for the existence of quadratic algebraic equations. From this, it can be asserted that the number of quadratic algebraic equations should come from the bifurcation number of the two-bifurcation topology.

Although the above assertion is summarized from the simplest two-bifurcation topology, it can be extended to higher-order topology [24], i.e., the third-order operator algebraic equation would be derived from three-bifurcation topology, etc. Generally, an n-order operator algebraic equation would be derived from n-bifurcation topology. In short, the bifurcation number always remains equal to the order of the operator algebraic equation. In topology, the bifurcation number is termed as the topological index. The topological index is an invariant that depicts topological characteristics, so it is also termed a topological invariant. Thus, a general proposition [24] holds below:

**Proposition 1.** *In physical fractal space, the order of fractal operator algebraic equations is always equal to the topological invariant of the fractal hypercell.*

This proposition portrays extremely the general invariant nature of physical fractal spaces. At this stage, we have thoroughly clarified the origin of the consistency in the literature [1–3]. Their physical laws all depend on the consistent physical fractal space form, and all have the fractal tree structure with two-bifurcation topology.

#### 5. The Universal Applicability of the Fractalization Ideology in Life Biological Systems

Although the above general proposition can be applied to higher-order topology, for living organisms, the topological index is usually 2, so order 1/2 should be sufficient. The reason is simple. Living organisms are completely controlled by the number 2; e.g., DNA is a double helix structure; cell division is always divided into two; the vascular tree is

two-bifurcation; and the neural tree is also two-bifurcation. In addition, there is also a common movement conversion related to the number 2, e.g., ratchet wheel movement. We found that the ratchet wheel motion in life can be mostly fractal, and its dynamics is mostly  $1/2$  order fractional dynamics. The ratchet wheel is a motion conversion mechanism in engineering (Figure 5). It is usually used to realize the conversion between two different motions, especially, converting a periodic (reciprocating) motion into a unidirectional (linear) motion. Because the phenomenon of motion conversion is widespread in nature and engineering, ratchet wheel motion has almost been extended to all disciplines. As long as the conversion between periodic motion and unidirectional motion is involved, there exists a ratchet wheel principle.

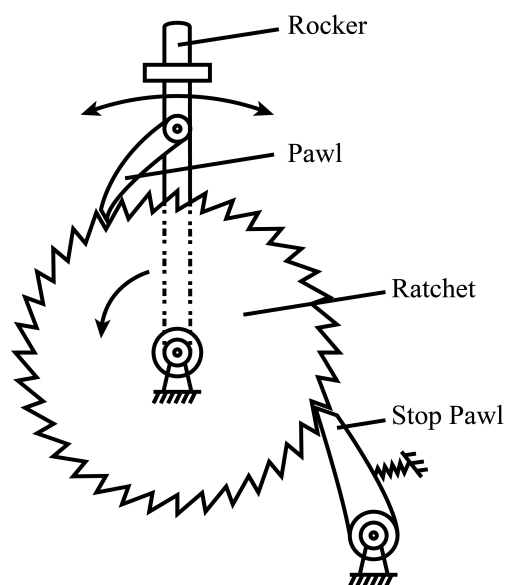


**Figure 5.** The principle diagram of ratchet wheel motion in engineering.

Almost all movements within the living body can be attributed to ratchet wheel movements. For example, the periodic systolic/diastolic beats of the heart drive the unidirectional flow of blood within the atria and ventricles. The cyclic systolic/diastolic moments of smooth muscle drive the unidirectional flow of lymphatic fluid. The regular movements of pulmonary respiration drive the unidirectional movement of gas exchange. It can be hypothesized that similar to the fractalization of blood flow images [3], there is also a fractalization of lymph flow images and gas exchange motion images. Similar to the  $1/2$ -order hemodynamics [3], there are also  $1/2$ -order lymphatic flow dynamics and gas exchange dynamics. To further corroborate the universality of the idea of fractalization within the living body, we then examine the interstitial fluid (ISF) flow throughout the body, specifically within the perivascular space (PVS) and within the perivascular and adventitial clearance (PAC), and we attempt to fractalize ISF flow.

Maiken et al. [25,26] showed that ISF flow was prevalent within the perivascular space (PVS) of cerebral arteries. Li et al. found that ISF flow was prevalent within the extravascular membrane [27] and that the flow direction was heart-oriented. Kong and Yu et al. demonstrated the existence of a flood-like flow of ISF within the gap around the vascular nerve bundle [28]. The accompanying arteries, veins, and nerves are encapsulated by a connective tissue membrane, forming a gap width of 500 to 2000 microns. The ISF flows along the gap toward the heart at a speed of about 1 cm/s. The heart-oriented character is essentially the unidirectional nature of the flow. Based on the centripetal metric, Yin et al. [29] proposed three laws for the ISF flow outside the vessel wall.

Maiken et al. [25,26] demonstrated that pulsation of the cerebral artery provides the driving force for the ISF flow within the perivascular space (PVS). The pulse-driven ISF flow can be attributed to ratchet wheel movements [30–33]: periodic diastole and contraction of

the arterial wall may cause periodic changes in the width of the PVS, which in turn drives two flows of ISF, a unidirectional flow in the axial direction and a diffuse flow in the radial direction into the brain parenchyma (Figure 6).

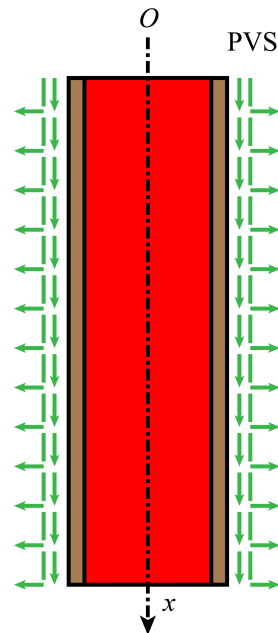


Figure 6. Images of ISF flow in the perivascular space (PVS).

Kong and Yu et al. [28] found in their experimental observations the ISF flow within the perivascular and adventitial clearances (PAC). The ISF flow within the PAC may be correlated with two movements. One is the pulsation of the artery and the other is the respiratory movements. Both movements may cause periodic changes in the width of the PAC. If we combine the above motion images with the three laws of ISF flow from the literature [29], we may attribute the ratchet wheel motion: the periodic changes in the width of the PAC may drive two flows of ISF, a heart-oriented flow along the axial direction, and a convergent flow into the PAC along the radially small vessel branches (Figure 7).

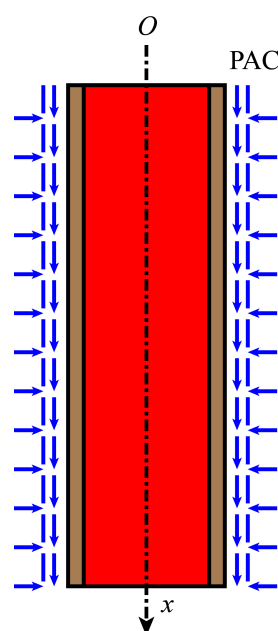
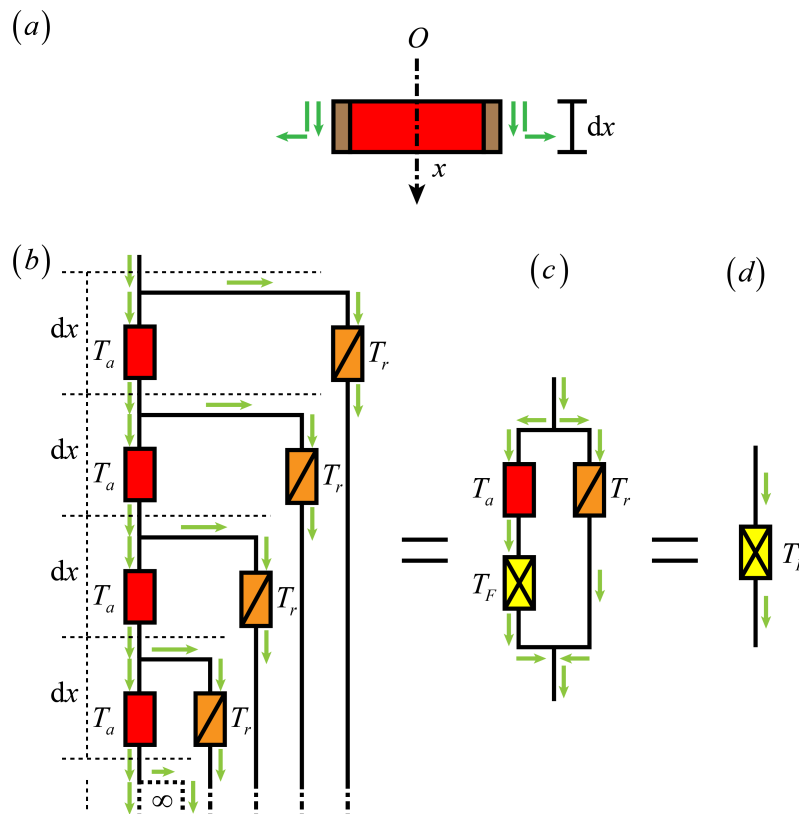


Figure 7. Images of ISF flow within the perivascular and adventitial clearances (PAC).

The flow images in Figures 6 and 7 have commonalities: they both are ratchet wheel movements, and both have two flows, one along the axial direction and the other along the radial direction. There are slight differences, i.e., the radial flows are in the opposite directions. Based on the commonality, the flow images in Figures 6 and 7 can be studied in a unified physical fractal space below. Figures 6 and 7 are very different from Figure 3. Figure 3 shows discrete molecular chains corresponding to discrete motion images, while Figures 6 and 7 show continuous flow images. However, there are commonalities between them. This will be shown in the following analysis. The focus will be on Figure 6. It is noted that the flow image in Figure 6 is very similar to the blood flow image in the literature [3]. In the literature [3], the fractalization of the blood flow image was achieved with the help of the infinitesimal differentiation idea. Similarly, the fractalization of the ISF flow image can also be achieved with the help of the infinite differential idea.

The PVS is divided into an infinite number of identical microcells  $dx$  along the axial direction. Similar to the literature [3], the physical elements controlling the flow on each microcell are examined to clarify the flow control operators. The control operator for axial flow per unit length is  $T_a$ , and the control operator for radial flow is  $T_r$ . Then, on each microcell, the operators  $T_a$  and  $T_r$  are connected in parallel with each other. Then, based on the continuity of flow between two adjacent microcells, the element (operator) fractal tree can be refined (Figure 8). It is noted that the fractal tree in Figure 8, with a topological index of 2, is both identical to the topology of the fractal tree in the literature [3] and identical to the topology of the fractal tree in Figure 3. The completely different subjects studied show complete consistency.



**Figure 8.** Fractalization of ISF flow within PVS or PAC. (a) Differential segment of infinite differential of physical image of ISF flow; (b) Infinite functional fractal tree structure of ISF flow; (c) Minimal representative cell in fractal tree of ISF; (d) Fractal element of ISF fractal tree.

Similarly, the fractal cell and fractal element can be abstracted from the fractal tree to define the fractal operator (Figure 8). The specific analysis procedure is omitted here. To this end, we achieved the fractalization of ISF flow images within the PVS. It is worth

noting that the above fractalization is specific to ISF flow within the PVS (Figure 6) but still holds for ISF flow within the PAC (Figure 7). As mentioned above, the differences between Figures 6 and 7 are the opposite radial flow directions. This also means that the signs of the control operators for their radial flows are opposite. In other words, there is a clear correspondence between the physical flow images of the ISF and the operator algebra after fractalization. Although the radial flow directions are different, both PVS and PAC are modulated by the two-bifurcation topological fractal tree structure, and thus, they have the same physical fractal space and kinetic law of motion. Based on the above analysis, it can be said that the dynamics of ISF flow in the living body is necessarily fractional dynamics with order  $1/2$ , and it is necessarily controlled by a fractal operator with order  $1/2$ .

## 6. Conclusions

Within the living organism, the idea of fractalization is universally applicable, fractal operators with order  $1/2$  universally exist, and fractional dynamics with order  $1/2$  play a decisive role. Such an assertion does not come from our subjective consciousness but from the universal structural form and kinematic form in living organisms themselves. The physical fractal spaces are abstract space forms that may not exist in reality. Infinity and self-identical equivalence within physical fractal space are completely idealized thought. Although not objectively real, they are still effective concepts for understanding nature and valid vocabulary for understanding life. The structures and motions of the living organisms are diverse. However, the two-bifurcation physical fractal space, without exception, adopts the simplest topology whose topological index is the smallest prime number, i.e., 2. This fact is an excellent reference for bionics, bionic materials science, and bionic structure science.

**Author Contributions:** Conceptualization, Y.Y., G.P. and J.G.; methodology, Y.Y., G.P. and J.G.; software, X.Y. and G.P.; validation, G.P., X.Y. and Y.K.; formal analysis, Y.Y., G.P. and J.G.; investigation, G.P., X.Y. and Y.K.; writing—original draft preparation, Y.Y.; writing—review and editing, G.P., X.Y. and Y.K. All authors have read and agreed to the published version of the manuscript.

**Funding:** This study was funded by the National Natural Science Foundation of China grant number 12050001 and 11672150.

**Institutional Review Board Statement:** Not applicable.

**Informed Consent Statement:** Not applicable.

**Data Availability Statement:** Not applicable.

**Conflicts of Interest:** The authors declare no conflict of interest related to this study.

## Abbreviations

The following abbreviations are used in this manuscript:

RHS	right-hand side
LHS	left-hand side
PVS	perivascular space
ISF	interstitial fluid
PAC	perivascular and adventitial clearance

## References

1. Guo, J.; Yin, Y.; Ren, G. Abstraction and operator characterization of fractal ladder viscoelastic hyper-cell for ligaments and tendons. *Appl. Math. Mech.* **2019**, *40*, 1429–1448. [[CrossRef](#)]
2. Guo, J.; Yin, Y.; Hu, X.; Ren, G. Self-similar network model for fractional-order neuronal spiking: Implications of dendritic spine functions. *Nonlinear Dyn.* **2020**, *100*, 921–935. [[CrossRef](#)]
3. Peng, G.; Guo, J.; Yin, Y. Self-Similar functional circuit models of arteries and deterministic fractal operators: Theoretical revelation for biomimetic materials. *Int. J. Mol. Sci.* **2021**, *22*, 12897. [[CrossRef](#)] [[PubMed](#)]
4. Zamir, M. Arterial branching within the confines of fractal L-system formalism. *J. Gen. Physiol.* **2001**, *118*, 267–276. [[CrossRef](#)] [[PubMed](#)]

5. Hapca, S.; Crawford, J.W.; MacMillan, K.; Wilson, M.J.; Young, I.M. Modelling nematode movement using time-fractional dynamics. *J. Theor. Biol.* **2007**, *248*, 212–224. [[CrossRef](#)]
6. Liu, F.; Burrage, K. Novel techniques in parameter estimation for fractional dynamical models arising from biological systems. *Comput. Math. Appl.* **2011**, *62*, 822–833. [[CrossRef](#)]
7. Kastelic, J.; Galeski, A.; Baer, E. Multicomposite structure of tendon. *Connect. Tissue Res.* **1978**, *6*, 11–23. [[CrossRef](#)]
8. Fan, J.; Liu, J.F.; He, J.H. Hierarchy of wool fibers and fractal dimensions. *Int. J. Nonlinear Sci. Numer. Simul.* **2008**, *9*, 293–296. [[CrossRef](#)]
9. Ji, B.; Gao, H. Mechanical properties of nanostructure of biological materials. *J. Mech. Phys. Solid.* **2004**, *52*, 1963–1990. [[CrossRef](#)]
10. Shen, Z.L.; Kahn, H.; Ballarini, R.; Eppell, S.J. Viscoelastic properties of isolated collagen fibrils. *Biophys. J.* **2011**, *100*, 3008–3015. [[CrossRef](#)]
11. Screen, H.R.C. Investigating load relaxation mechanics in tendon. *J. Mech. Behav. Biomed. Mater.* **2008**, *1*, 51–58. [[CrossRef](#)] [[PubMed](#)]
12. Xu, G.; Gong, L.; Yang, Z.; Liu, X.Y. What makes spider silk fibers so strong? From molecular-crystallite network to hierarchical network structures. *Soft Matter*. **2014**, *10*, 2116–2123. [[CrossRef](#)] [[PubMed](#)]
13. Chaudhuri, R.; Knoblauch, K.; Gariel, M.A.; Kennedy, H.; Wang, X.J. A large-scale circuit mechanism for hierarchical dynamical processing in the primate cortex. *Neuron* **2015**, *88*, 419–431 [[CrossRef](#)] [[PubMed](#)]
14. Joglekar, M.R.; Mejias, J.F.; Yang, G.R.; Wang, X.J. Interareal balanced amplification enhances signal propagation in a large-scale circuit model of the primate cortex. *Neuron* **2018**, *98*, 222–234.e8. [[CrossRef](#)]
15. Burattini, R.; Gnudi, G. Computer identification of models for the arterial tree input impedance: Comparison between two new simple models and first experimental results. *Med. Biol. Eng. Comput.* **1982**, *20*, 134–144. [[CrossRef](#)]
16. Abdolrazaghi, M.; Navidbakhsh, M.; Hassani, K. Mathematical modelling of intra-aortic balloon pump. *Comput. Method. Biomech.* **2010**, *13*, 567–576. [[CrossRef](#)]
17. Goldwyn, R.M.; Watt, T.B. Arterial pressure pulse contour analysis via a mathematical model for the clinical quantification of human vascular properties. *IEEE Trans. Bio-Med. Eng.* **1967**, *BME-14*, 11–17. [[CrossRef](#)]
18. Petruska, J.A.; Hodge, A.J. A subunit model for the tropocollagen macromolecule. *Proc. Natl. Acad. Sci. USA* **1964**, *52*, 1963–1990. [[CrossRef](#)]
19. Fratzl, P. Cellulose and collagen: from fibres to tissues. *Curr. Opin. Colloid Interface Sci.* **2003**, *8*, 32–39. [[CrossRef](#)]
20. Mandelbrot, B. How long is the coast of Britain? Statistical self-similarity and fractional dimension. *Science* **1967**, *156*, 636–638. [[CrossRef](#)]
21. Yang, F.; Zhu, K. Q. On the definition of fractional derivatives in rheology. *Theor. Appl. Mech. Lett.* **2011**, *1*, 12007. [[CrossRef](#)]
22. Mikusinski, J. *Operational Calculus*, 2nd ed.; Pergamon Press: Oxford, UK, 1983.
23. Hu, K.X.; Zhu, K.Q. Mechanical analogies of fractional elements. *Chin. Phys. Lett.* **2009**, *26*, 108301.
24. Yin, Y.; Peng, G.; Yu, X. Algebraic equations and non-integer orders of fractal operators abstracted from biomechanics. *Acta Mech. Sin.* **2022**, *38*, 521488. [[CrossRef](#)]
25. Iliff, J.J.; Wang, M.; Liao, Y.; Plogg, B.A.; Peng, W.; Gundersen, G.A.; Benveniste, H.; Vates, G.E.; Deane, R.; Goldman, S.A.; et al. A paravascular pathway facilitates CSF flow through the brain parenchyma and the clearance of interstitial solutes, including amyloid  $\beta$ . *Sci. Transl. Med.* **2012**, *4*, 147. [[CrossRef](#)] [[PubMed](#)]
26. Mestre, H.; Tithof, J.; Du, T.; Song, W.; Peng, W.; Sweeney, A.M.; Olveda, G.; Thomas, J.H.; Nedergaard, M.; Kelley, D. H. Flow of cerebrospinal fluid is driven by arterial pulsations and is reduced in hypertension. *Nat. Commun.* **2018**, *9*, 4878. [[CrossRef](#)] [[PubMed](#)]
27. Li, H.; Yang, J.; Chen, M.; Xu, L.; Wang, W.; Wang, F.; Tong, J.; Wang, C. Visualized regional hypodermic migration channels of interstitial fluid in human beings: Are these ancient meridians? *J. Altern. Complement. Med.* **2018**, *14*, 621–628. [[CrossRef](#)]
28. Kong, Y.; Yu, X.; Wang, F.; Yin, Y. Interstitial fluid flows along perivascular and adventitial clearances around neurovascular bundles. *to be submitted*.
29. Yin, Y.; Li, H.; Peng, G.; Yu, X.; Kong, Y. Fundamental kinematics laws of interstitial fluid flows on vascular walls. *Theor. Appl. Mech. Lett.* **2021**, *11*, 100245. [[CrossRef](#)]
30. Wang, P.; Olbricht, W.L.; Fluid mechanics in the perivascular space. *J. Theor. Biol.* **2011**, *274*, 52–57. [[CrossRef](#)]
31. Yokoyama, N.; Takeishi, N.; Wadad, S. Cerebrospinal fluid flow driven by arterial pulsations in axisymmetric perivascular spaces: Analogy with Taylor’s swimming sheet. *J. Theor. Biol.* **2021**, *523*, 110709. [[CrossRef](#)] [[PubMed](#)]
32. Bilston, L.E.; Fletcher, D.F.; Brodbelt, A.R.; Stoodley, M.A. Arterial pulsation-driven cerebrospinal fluid flow in the perivascular space: a computational model. *Comput. Methods Biomech. Biomed. Eng.* **2003**, *6*, 235–241. [[CrossRef](#)]
33. Bilston, L.E.; Martinac, A.D. Computational modelling of fluid and solute transport in the brain. *Biomech. Model. Mechanobiol.* **2020**, *19*, 781–800.